

# Dip-coating on TiO<sub>2</sub> foams using a suspension of Pt–TiO<sub>2</sub> nanopowder synthesized by laser pyrolysis—preliminary evaluation of the catalytic performances of the resulting composites in deVOC reactions

Sophie Giraud<sup>a,\*</sup>, Guillaume Loupias<sup>a</sup>, Hicham Maskrot<sup>b</sup>, Nathalie Herlin-Boime<sup>b</sup>, Sabine Valange<sup>c</sup>, Erwan Guélou<sup>c</sup>, Joël Barrault<sup>c</sup>, Zelimir Gabelica<sup>d</sup>

<sup>a</sup> CEA-Saclay, DRT/DTNM/LTMEX, F-91191 Gif sur Yvette Cedex, France

<sup>b</sup> CEA-Saclay, DSM/DRECAM/SPAM/LFP, CEA/CNRS URA 2453, F-91191 Gif sur Yvette Cedex, France

<sup>c</sup> LACCO, UMR CNRS 6503, ESIP, 40 Av. Recteur Pineau, F-86022 Poitiers, France

<sup>d</sup> UHA-ENSCMu, GSEC, 3, Rue A. Werner, F-68903 Mulhouse Cedex, France

Available online 6 June 2006

## Abstract

As an extension of a study to generate ceramic-metal nanosized composites further deposited on ceramic foams, here we describe a new route to prepare Pt–TiO<sub>2</sub> nanopowders of controlled metallic size and their further coating of TiO<sub>2</sub> foams. Their efficiency as catalysts in volatile organic compound elimination (deVOC) reactions was evaluated and compared to those of the corresponding classical unsupported mixed powders.

Composite metal/ceramic nanopowders (Pt–TiO<sub>2</sub>) were synthesized by laser pyrolysis using organo-metallic precursors. Successive dip-coatings on TiO<sub>2</sub> foams with aqueous slurries of nanodispersed Pt–TiO<sub>2</sub> particles were then achieved. Both foam-supported and unsupported Pt–TiO<sub>2</sub> grains of about 20 nm could be stabilized, confirming no significant particles coalescence after a thermal treatment at 460 °C. Both proved equally efficient catalysts for the total oxidation of methanol, selected as probe deVOC reaction, thereby demonstrating that the dispersion of the nanopowders over the preformed ceramics does not modify their catalytic performances.

© 2006 Elsevier Ltd. All rights reserved.

**Keywords:** Laser pyrolysis; Composites

## 1. Introduction

Among the huge range of applications of nanostructured materials, catalysis and in particular environmental catalysis i.e. new processes for green chemistry, is a privileged domain of applications. In this field, the emission of volatile organic compounds (VOC) is an important environmental problem and more efficient processes and catalysts are needed to eliminate such products from various effluents. Due to the high surface of the nanostructured materials, good catalytic properties can be expected. Indeed, a high dispersion of the active phase (oxide, metal) and its adequate retention on the support strongly increase the catalytic efficiency as well as the durability of the solids. The catalyst performance could be improved by e.g. controlling the dispersion and the stability of the active nanophases on a high surface (macroporous) supports.

Nanoparticles with well defined chemical composition, size and structure<sup>1–3</sup> and a high specific surface can be obtained by the laser pyrolysis method. This method is based on the interaction of a powerful IR laser beam with a mixture of gaseous or liquid precursors, one of them absorbing the laser radiation. The temperature increases rapidly, leading to the decomposition of the precursors. An incandescent flame is observed in the interaction zone where nanoparticles nucleate and grow. The residence time adjusted by the carrier gas flow allows the control of the nanoparticle size. Their chemical composition depends on the nature and the content of the different reagents in the precursor mixture.

In this paper, we present the extension of the laser pyrolysis method to the synthesis of an active composite Pt–TiO<sub>2</sub> for catalytic applications. Pure TiO<sub>2</sub> nanopowders were already obtained by laser pyrolysis from various liquid precursors such as: titanium isopropoxide (TTIP), Ti(OC<sub>3</sub>H<sub>7</sub>)<sub>4</sub><sup>4,5</sup> or titanium ethoxide Ti(OC<sub>2</sub>H<sub>5</sub>)<sub>4</sub>.<sup>4</sup> Doped TiO<sub>2</sub> nanopowders (Mo, W, Al, Ga) were also prepared by laser pyrolysis from TTIP

\* Corresponding author. Tel.: +33 1 69 08 25 14; fax: +33 1 69 08 82 52.  
E-mail address: [sophie.giraud@cea.fr](mailto:sophie.giraud@cea.fr) (S. Giraud).

precursor.<sup>6,7</sup> However, to our knowledge, the synthesis of Pt doped TiO<sub>2</sub> by laser pyrolysis has not yet been reported.

In that paper, we present:

- a one step preparation of nanopowders of platinum well dispersed over TiO<sub>2</sub> (Pt–TiO<sub>2</sub> composite nanopowders) by laser pyrolysis;
- the further coating of such powders on a ceramic (TiO<sub>2</sub>) foam using a simple procedure, yielding Pt–TiO<sub>2</sub>/TiO<sub>2</sub> foam-composites;
- the performances of those composite materials (nanopowders and foam-composites) for catalytic methanol oxidation (deVOC).

## 2. Experimental

### 2.1. Pt–TiO<sub>2</sub> preparation

The Pt–TiO<sub>2</sub> nanopowders were synthesized by laser pyrolysis using TTIP as Ti precursor.<sup>4,5</sup> The solution containing the precursors was prepared using a procedure very similar to the one described by Ströbel,<sup>8</sup> by first dissolving appropriate amounts of platinum acetylacetonate Pt(Acac) (Aldrich, 97%) in a xylene (Aldrich, 98%)/ethylacetate (SDS, purum) mixture (65:35 vol/vol) and then mixing it with TTIP (Aldrich, 97%). Nevertheless such mixture absorbs weakly the laser radiation so ethylene C<sub>2</sub>H<sub>4</sub> was added as sensitizer gas. In the experiments reported here, the aerosol droplets were carried out in an argon flow (21 min<sup>-1</sup>) into the reaction chamber through a 6 mm in diameter nozzle.

### 2.2. Pt–TiO<sub>2</sub> deposition on TiO<sub>2</sub> foams

TiO<sub>2</sub> is widely used as photocatalyst as suggested by the prolific literature on the subject.<sup>9–18</sup> Suspensions of TiO<sub>2</sub> often are aqueous.<sup>11–14,16,17</sup> So an aqueous suspension of Pt–TiO<sub>2</sub> was prepared at a concentration of 10 g/l. The powder tended to be slightly hydrophobic and had to be ground in a mortar with a small quantity of water prior the addition of all the water. It was sonicated in order to obtain a good dispersion of the nanopowder.

Ceramic foams made of TiO<sub>2</sub> (20 ppi) were provided by the CTI company (France), which is involved in the NACACOMO program. They were cleaned in warm water, ethanol and then dried. Multiple layers of Pt–TiO<sub>2</sub> have been deposited on each TiO<sub>2</sub> substrate. After each dip into the colloidal suspension, the samples were dried in air at room temperature, then heated at 80 °C. After 3–6 dips, a thermal treatment was carried out in air at 460 °C during 3 h. After every operation, the samples were carefully and precisely weighed.

### 2.3. Characterization

Chemical analyses were performed using conventional methods (CNRS analytical center/Solaize-France) with a relative uncertainty of ±2% for C, O, and of ±3% for Pt, Ti determination. Specific surface area ( $S_{\text{BET}}$ ) was measured by the

BET method using a Micromeritics Flowsorb 2300 instrument. Powder density ( $\rho$ ) was measured by Helium pycnometry (Micromeritics AccuPyc 1330). An equivalent diameter ( $D$ ) was deduced from  $S_{\text{BET}}$  and  $\rho$ , assuming spherical shape particles. The size of the grains dispersed in water was obtained from photo correlation spectroscopy (PCS) using a Malvern HS1000 apparatus. An X-ray diffraction (XRD) powder pattern was obtained with an automated diffractometer (Philips, APD1700) using the Cu K $\alpha$  radiation and the crystallite size was evaluated using the well-known Scherrer equation.

The electrophoretic mobility of the suspension was studied as a function of pH. The measurements were carried out with a Delsa 440 instrument (Beckman Coulter). Aqueous dispersions of pure TiO<sub>2</sub> (P25 from Degussa), used as reference, and the above synthesized Pt–TiO<sub>2</sub> nanoparticles were prepared at a concentration of 0.2 g l<sup>-1</sup>. The pH was monitored with NaOH 0.1 M and HCl 0.1 M. A salt, KCl, was used as electrolyte at concentrations of 10<sup>-2</sup> and 10<sup>-3</sup> M.

Microstructural analyses were performed using a TEM instrument (JEOL 2000FX, 200 kV) for the powder (after a heat treatment at 460 °C) and a FE-SEM apparatus (LEO-1530) for the deposits. The surface of Pt–TiO<sub>2</sub> particles as well as the Pt particle size analysis were investigated by TEM (Philips CM120 microscope, equipped with a LaB6 filament at 120 kV) coupled to an EDX analyser (fixed probe). Electron microdiffraction patterns were also recorded to identify the nature of the platinum-bearing particles. The samples were at first occluded in a resin that was cut into sections of 30–50 nm with a microtome equipped with a diamond cutter, before they were supported on a carbon-coated nickel grid.

H<sub>2</sub>-chemisorption was performed by using a Micromeritics AutoChem 2910 instrument. The sample was first reduced under H<sub>2</sub> at 450 °C during 8 h, and then purged by an Ar flow for 6 h at 450 °C. H<sub>2</sub>-chemisorption was performed using a dynamic pulse method at ambient temperature with a loop gas of 5% H<sub>2</sub>–Ar until the integrated areas of consecutive pulses were constant.

### 2.4. Catalytic tests: methanol oxidation

Such studies required the use of an isothermal flow reactor able to work semi-automatically, in order to provide highly reproducible results. The method used was described elsewhere.<sup>19</sup>

The gaseous mixture used for the reaction consisted of oxygen and methanol vapor, diluted by helium. The methanol flow rate was managed by using a ‘saturator’, containing a hot (60–80 °C) methanol solution through which the O<sub>2</sub>–He mixture was bubbling. The final composition of the feed is controlled by the methanol partial pressure by means of a condenser in which the temperature of the circulating cooling fluid was fixed by a cryostat at 11 °C. The catalytic reactor consists of a straight Pyrex glass tube where the catalyst is held by two quartz wool plugs.

A sample loop connected to a ten-port valve allows to inject into a gas chromatograph (GC) either a known volume of the gas mixture from the reactor, or the reactant feed (by-pass position). The sample loops are connected so as to inject into the GC

analyzer (involving a column packed with chromosorb 107) a known volume (0.5 ml for the FID), either of the reactant feed or of the gas mixture. A computerized system was used for the acquisition and treatment of the chromatograms. The apparatus allowed the accurate measurement of the surface area of the formaldehyde peak down to a value corresponding to a yield of 0.5%, for an initial methanol concentration of 7.7%.

### 3. Results and discussion

#### 3.1. Characterization of the powder

The results of the Pt–TiO<sub>2</sub> nanopowder characterization (particle size and composition) are presented in Table 1. It must be noted that the Pt/Ti ratios in solution and in the resulting powder are similar. A satisfactory agreement is observed between the grain size measured by BET or PCS in suspension which indicates a good dispersion of the nanopowders. Chemical analyses show that the powder contains a small amount of free carbon, probably stemming from a partial cracking of ethylene<sup>5</sup> and/or the decomposition of the secondary products. It is totally eliminated after heat treatment under air at 400 °C during 3 h. The XRD pattern (not shown here) corresponds to a mixture of phases involving a major anatase phase and a small amount of rutile. During the synthesis of TiO<sub>2</sub> by laser pyrolysis, anatase is usually the only crystalline phase that forms although increasing percentages of rutile were observed at higher reaction temperature.<sup>5</sup> In a previous case, it has been suggested<sup>20</sup> that the formation of a rutile phase was promoted by the formation of PtO<sub>2</sub> whose structure is similar to that of rutile. Particle sizes range between 15 and 20 nm (TEM image, Fig. 1), which is in agreement with the calculated equivalent diameter. Very few aggregates of around 55 nm were observed. Fig. 2 shows a better resolved TEM image of Pt–TiO<sub>2</sub> with platinum particles

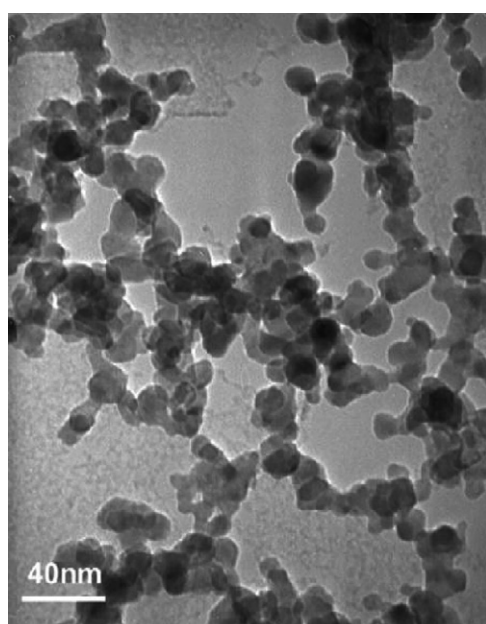


Fig. 1. TEM of the Pt–TiO<sub>2</sub> nanopowder after a thermal treatment at 460 °C.

Table 1  
Main experimental parameters and characterization of Pt–TiO<sub>2</sub> nanoparticles

Powder	C <sub>2</sub> H <sub>4</sub> flow (cm <sup>3</sup> min <sup>-1</sup> )	Pt/Ti ratio (wt.%) solution	Pt/Ti ratio (wt.%) powder	Pt/(Pt–TiO <sub>2</sub> ) ratio (wt.%)	S <sub>BET</sub> <sup>a</sup> (m <sup>2</sup> g <sup>-1</sup> )	Density <sup>a</sup> ρ (g cm <sup>-3</sup> )	Particle equivalent diameter D <sub>BET</sub> (nm)	Particle hydrodynamic diameter <sup>a</sup> D <sub>PCS</sub> (nm)	Particle TEM diameter (nm)	XRD crystal size D <sub>XRD</sub> (nm)
Pt–TiO <sub>2</sub>	800	0.9	0.9	0.54	92	3.7	17.6	24	15–20	10

<sup>a</sup> On powder heated at 400 °C/3 h.

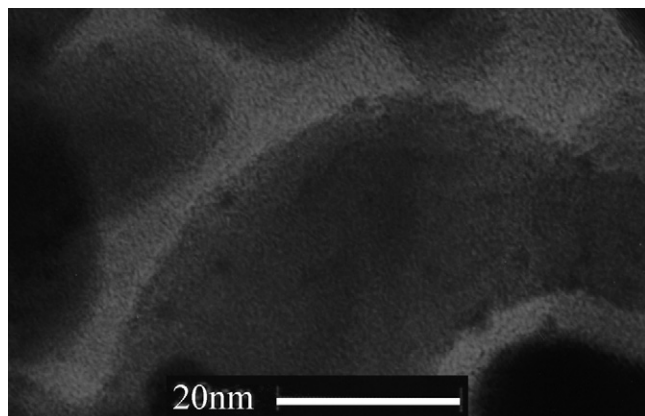


Fig. 2. TEM of the Pt–TiO<sub>2</sub> nanopowder, localization of Pt particles. Reprinted from Catalysis Today; H. Maskrot, Y. Leconte, N. Herlin-Boime, C. Reynaud, E. Guelou, L. Pinard, S. Valange, J. Barrault; Synthesis of nanostructured catalysts by laser pyrolysis; to be published; copyright (2006), with permission from Elsevier.

of 2–3 nm diameter (which appear darker on Fig. 2), lying on the TiO<sub>2</sub> surface. From this morphological point of view, the Pt–TiO<sub>2</sub> nanopowders obtained by laser pyrolysis appear very similar to the Pt–TiO<sub>2</sub> nanoparticles obtained by the flame synthesis method.<sup>21</sup>

From H<sub>2</sub>-chemisorption, a Pt dispersion value of 45% is measured which indicates a mean platinum particle size of 2.6 nm, in good agreement with the value evaluated by TEM (Fig. 2).

The electrophoretic mobility is a function of both pH and ionic strength of the suspension; hence it is important to carefully monitor/control these parameters. The mobility (and therefore the zeta potential) of a suspension is directly related to the magnitude of the repulsive force between the particles. The greater the zeta potential the greater the repulsive force, therefore the lower the probability of aggregating particles. Knowing the isoelectric point (pH<sub>iep</sub>) allows an easy recovery of the flocculated powder; thereby preventing an undesired dispersion of the nanopowders in the environment. As a consequence, in a pH zone far from the pH<sub>iep</sub>, it is expected that the surface charges are sufficient to induce a repulsive force between the particles, leading to well dispersed suspensions. The solid loading can also influence the particle behavior. Fig. 3 shows the electrophoretic mobility versus pH and ionic strength for TiO<sub>2</sub>–P25 and Pt–TiO<sub>2</sub>. At pH < pH<sub>iep</sub>, the surface is positively charged, the positive sign of the mobility being due to the adsorption of H<sup>+</sup> onto the surface; conversely at high pH, protons are released from the surface, which explains the negative sign of the mobility.

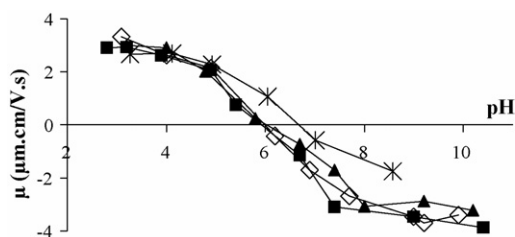


Fig. 3. Electrophoretic mobility vs. pH for TiO<sub>2</sub> P25 (\*) and for Pt–TiO<sub>2</sub> (◇) without electrolyte; ▲ and ■ with KCl respectively, 10<sup>−2</sup> and 10<sup>−3</sup> M.

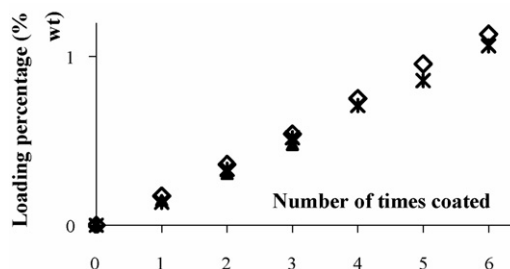


Fig. 4. Evolution of the Pt–TiO<sub>2</sub> loading (wt.%) vs. the number of dippings for three TiO<sub>2</sub> ceramic foams.

The pH<sub>iep</sub> (zero electrolyte concentration) of the TiO<sub>2</sub>–P25 dispersions (pH<sub>iep</sub> = 6.7) is in good agreement with the literature values.<sup>22–25</sup> The pH<sub>iep</sub> of the Pt–TiO<sub>2</sub> suspensions are obtained at 6, independently of the presence of electrolyte (KCl). The ions (K<sup>+</sup> and Cl<sup>−</sup>) added have a slight effect on the electrokinetic measurements, they allow us to evaluate the zeta potential using the Smoluchowski equation.<sup>26</sup>

### 3.2. Pt–TiO<sub>2</sub> nanopowder deposition on TiO<sub>2</sub> foam

The prepared suspension of Pt–TiO<sub>2</sub> (10 g/l) tends to be naturally acidic (pH around 4) so that it was decided to work at this acidic pH which is far enough from the pH<sub>iep</sub>. Ceramic foams were dipped in this stable suspension. The wt.% of catalyst immobilized increases linearly with the number of dippings (Fig. 4). The different slopes of the straight lines are due to the differences in the ceramic support surfaces. A weight loss observed during the thermal treatment illustrates the elimination of the carbonaceous species formed during pyrolysis.

Fig. 5a shows the structure (texture) of the ceramic foam used as support. Such texture is still well detectable after three dips followed by a thermal treatment (Fig. 5b). No important grain growth was observed (Fig. 5c) after annealing. The particle size is still in the nanometric range.

### 3.3. Catalysis: methanol oxidation

The preliminary catalytic results in methanol oxidation over Pt–TiO<sub>2</sub> nanopowders and their coating on ceramic TiO<sub>2</sub> foams are presented in Table 2. The ability of all the samples to favor the total elimination of methanol into CO<sub>2</sub> was evaluated and compared at 50% conversion.

The Pt–TiO<sub>2</sub> nanopowder synthesized by laser pyrolysis (0.54 wt.% Pt) was compared to a Pt/SiO<sub>2</sub> reference catalyst involving a similar Pt content (0.4 wt.% Pt). This Pt reference solid was prepared through a classical impregnation of a commercial silica (Aerosil D200, Degussa) with an aqueous solution of diamminodinitroplatinum(II), [Pt(NH<sub>3</sub>)<sub>2</sub>(NO<sub>2</sub>)<sub>2</sub>]. After impregnation, the solid was left to evaporate and dried at 100 °C in an oven, before annealing in air flow at 450 °C for 4 h.

The catalytic results reveal that the Pt–TiO<sub>2</sub> nanopowder synthesized by laser pyrolysis is more active than a conventional Pt/SiO<sub>2</sub> catalyst for the complete methanol decomposition into CO<sub>2</sub>. Indeed, the methanol oxidation (50% conversion) over



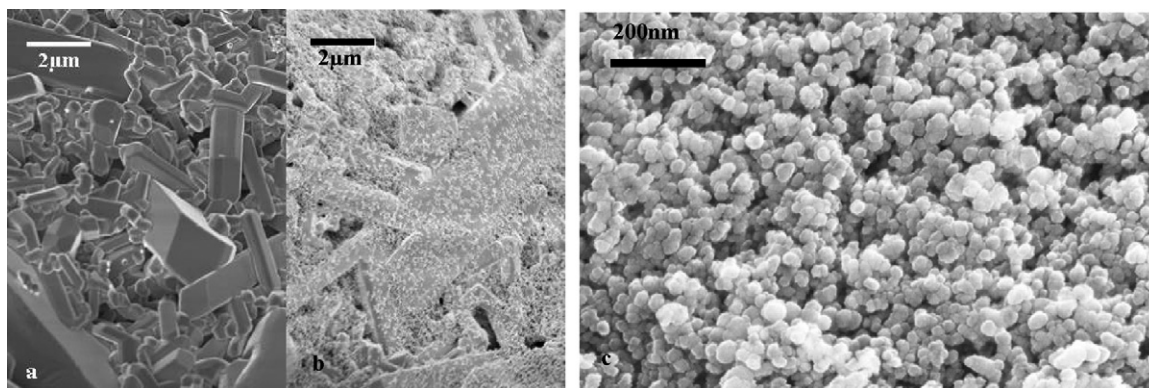


Fig. 5. Microstructure of the ceramic foam (a) before dipping; (b) after three dips and (c) after six dips, in the Pt–TiO<sub>2</sub> suspension (FE-SEM).

Pt–TiO<sub>2</sub> nanopowders occurs at a lower temperature (80 °C instead of 115 °C) than for Pt/SiO<sub>2</sub>. This interesting result clearly demonstrates the possibility to generate by laser pyrolysis nanometric platinum particles well dispersed within the TiO<sub>2</sub> substrate, that reveal very active and selective in the total oxidation of MeOH into CO<sub>2</sub>.

The next step consisted in evaluating the catalytic performances of a TiO<sub>2</sub> ceramic foam coated with Pt–TiO<sub>2</sub> nanopowders (Pt–TiO<sub>2</sub>/TiO<sub>2</sub> foam-composites). The catalytic tests were first performed on the crushed ceramic composites, for a direct comparison with the nanopowders, then on the as prepared foam monoliths. It was first necessary to determine the MeOH oxidation theoretical temperatures at 50% conversion in order to check the absence of catalytic activity loss during the coating process.

These temperatures were determined by taking into account the Arrhenius law for a methanol activation energy ( $E_a$ ) equal to 85 KJ mol<sup>-1</sup>, considering as a reference the result obtained at 50% conversion for Pt–TiO<sub>2</sub> nanopowder synthesized by laser pyrolysis (see below).

$$K = A e^{-E_a/RT}$$

$$\ln \left[ \frac{(1 - 0.5)}{(0.5)\tau'} \right] = -\ln A + E_a/RT$$

considering that  $\tau'$  is equal to the ratio of the amount of active metal and the flow rate

$$\tau' = m/Q \text{ with } m = \text{catalyst mass} \times \% \text{ metal}$$

$$\ln m - \ln Q = -\ln A + E_a/RT$$

The results (Table 2) indicated that the temperatures measured for the total oxidation of methanol are similar to those evaluated by taking into account the Arrhenius law, independently on the number of dippings.

The volatile organic compound elimination (deVOC) tests performed on these composites demonstrate that the dispersion of the nanopowders over the preformed ceramic does not modify their catalytic performances, thereby confirming that the dipping method used to coat the foam monoliths does not alter the active sites of the nanopowders synthesized by laser pyrolysis. The Pt–TiO<sub>2</sub> nanopowders and their coating onto ceramic foams therefore lead to very efficient catalysts for the total decomposition of methanol thereby showing that the shaping of these materials could be envisaged for industrial applications.

#### 4. Conclusions

Laser pyrolysis allowed the preparation in one step of Pt–TiO<sub>2</sub> nanopowders, thereby demonstrating its potentiality as

Table 2

Preliminary catalytic results in methanol oxidation into CO<sub>2</sub> over Pt–TiO<sub>2</sub> nanopowders, over Pt–TiO<sub>2</sub>/TiO<sub>2</sub> foam-composites and over a Pt/silica reference solid

Catalyst	Sample weight (mg)	Pt (wt.%)	$T$ (°C) <sup>a</sup> theoretical	$T$ (°C) at 50% methanol conversion
Pt/SiO <sub>2</sub> (Ref.)	50	0.4	–	115
Pt–TiO <sub>2</sub>	50	0.54	–	80
Pt–TiO <sub>2</sub> /TiO <sub>2</sub> foam-composite, (3 dippings) (crushed)	50	$0.231 \times 10^{-2b}$	160	175
Pt–TiO <sub>2</sub> /TiO <sub>2</sub> foam-composite, (3 dippings) (monolith)	380	$0.231 \times 10^{-2b}$	125	125
Pt–TiO <sub>2</sub> /TiO <sub>2</sub> foam-composite, (6 dippings) (crushed)	50	$0.532 \times 10^{-2b}$	150	165
Pt–TiO <sub>2</sub> /TiO <sub>2</sub> foam-composite, (6 dippings) (monolith)	450	$0.532 \times 10^{-2b}$	110	115

<sup>a</sup> MeOH oxidation temperatures determined by taking into account the Arrhenius law ( $E_a = 85 \text{ KJ mol}^{-1}$ ) over Pt–TiO<sub>2</sub> nanopowders synthesized by laser pyrolysis as a reference (see text).

<sup>b</sup> The Pt content was theoretically evaluated from the number of dippings, considering the total mass of the composite (ceramic foam coated by Pt–TiO<sub>2</sub> nanopowders).

an original, versatile and efficient method for catalyst preparation. Such solids proved very efficient in catalyzing methanol oxidation into CO<sub>2</sub>, showing their potentiality in being more widely used for the total oxidation of volatile organic compounds (deVOC).

The further deposition of Pt–TiO<sub>2</sub> nanopowders over TiO<sub>2</sub> ceramic foams by successive dippings led to Pt–TiO<sub>2</sub> (nanopowders)/TiO<sub>2</sub> (foam monolith)-composites that proved as active in MeOH oxidation as the initial Pt–TiO<sub>2</sub> phase but much easier to handle on a large scale in various industrial processes. Work is in progress to extend this original preparation method to other catalytic composites.

### Acknowledgements

This work was supported by the French Ministry of Economy, Finance and Industry (MINEFI) under the NACACOMO consortium. The authors gratefully acknowledge Yvette Dextre (CEA) for the FE-SEM measurements, Cécile Genevois (CEA) for the TEM images and Stéphane Pronier (Université de Poitiers) for recording combined TEM-EDX analyses and for constructive discussions.

### References

1. Cannon, W. R., Danforth, S. C., Haggerty, J. S. and Marra, R. A., Sinterable ceramic powders from laser-driven reactions: ii powder characteristics and process variables. *J. Am. Ceram. Soc.*, 1986, **65**(7), 324–330.
2. Cauchetier, M., Croix, O., Herlin, N. and Luce, M., Nanocomposite Si/C/N powder production by laser-aerosol interaction. *J. Am. Ceram. Soc.*, 1994, **77**(4), 993–998.
3. Herlin, N., Armand, X., Musset, E., Martinengo, H., Luce, M. and Cauchetier, M., Nanometric Si-based oxide powders: synthesis by laser spray pyrolysis and characterization. *J. Eur. Ceram. Soc.*, 1996, **16**(10), 1063–1073.
4. Casey, J. D. and Haggerty, J. S., Laser-induced vapour-phase synthesis of titanium dioxide. *J. Mater. Sci.*, 1987, **22**(12), 4307–4312.
5. Curcio, F., Musci, M., Notaro, N. and De Michele, G., Synthesis of ultra-fine TiO<sub>2</sub> powders by a CW CO<sub>2</sub> laser. *Appl. Surf. Sci.*, 1990, **46**, 225–229.
6. Bregani, F., Casale, C., Depero, L. E., Natali-Sora, I., Robba, D., Sangaletti, L. and Toledo, G. P., Temperature effects on the size of anatase crystallites in Mo–TiO<sub>2</sub>/and W–TiO<sub>2</sub> powders. *Sens. Actuators B*, 1996, **31**, 25–28.
7. Depero, L. E., Marino, A., Allieri, B., Bontempi, E., Sangaletti, L., Casale, C. and Notaro, M., Morphology and microstructural properties of TiO<sub>2</sub> nanopowders doped with trivalent Al and Ga cations. *J. Mater. Res.*, 2000, **15**(10), 2080–2086.
8. Strobel, R., Stark, W. J., Mädler, L., Pratsinis, S. E. and Baiker, A., Flame-made platinum/alumina: structural properties and catalytic behaviour in enantioselective hydrogenation. *J. Catal.*, 2003, **213**, 296–304.
9. Tanaka, T., Teramura, K., Yamamoto, T., Takenaka, S., Yoshida, S. and Funabiki, T., TiO<sub>2</sub>/SiO<sub>2</sub> photocatalysts at low levels of loading: preparation, structure and photocatalysis. *J. Photochem. Photobiol. A: Chem.*, 2002, **148**, 277–281.
10. Yang, P., Lu, C., Hua, N. and Du, Y., Titanium dioxide nanoparticles co-doped with Fe<sup>3+</sup> and Eu<sup>3+</sup> ions for photocatalysis. *Mater. Lett.*, 2002, **57**, 794–801.
11. Byrne, J. A., Eggins, B. R., Brown, N. M. D., McKinney, B. and Rouse, M., Immobilisation of TiO<sub>2</sub> powder for the treatment of polluted water. *Appl. Catal. B: Environ.*, 1998, **17**, 25–36.
12. Ray, A. K. and Beenackers, A. A. C. M., Novel photocatalytic reactor for water purification. *AIChE J.*, 1998, **44**(2), 477–483.
13. Bideau, M., Claudel, B., Dubien, C., Faure, L. and Kazouan, H., On the ‘immobilization’ of titanium dioxide in the photocatalytic oxidation of spent waters. *J. Photochem. Photobiol. A: Chem.*, 1995, **91**, 137–144.
14. Vinodgopal, K. and Kamat, P. V., Enhanced degradation of an azo dye using SnO<sub>2</sub>/TiO<sub>2</sub> coupled semiconductor thin films. *Environ. Sci. Technol.*, 1995, **29**, 841–845.
15. Nair, M., Luo, Z. and Heller, A., Rates of photocatalytic oxidation of crude oil on salt water on buoyant, cenosphere-attached titanium dioxide. *J. Electrochem. Soc.*, 1993, **32**, 2318–2323.
16. Matthews, R. W., Photooxidative degradation of coloured organics in water using supported catalysts TiO<sub>2</sub> on sand. *Water Res.*, 1991, **25**(10), 1169–1176.
17. Mills, A., Worsley, D. and Davies, R. H., Effect of pH on the stability of TiO<sub>2</sub> coatings on glass photocatalysis reactors for water purification. *J. Chem. Soc., Chem. Commun.*, 1994, 2677–2678.
18. Jackson, N. B., Wang, C. M., Luo, Z., Schwitzgebel, J., Ekerdt, J. G., Brock, J. R. and Heller, A., Attachment of TiO<sub>2</sub> powders to hollow glass microbeads: activity of the TiO<sub>2</sub>-coated beads in the photo-assisted oxidation of ethanol to acetaldehyde. *J. Electrochem. Soc.*, 1991, **138**(12), 3660–3664.
19. Tatibouet, J. M., Methanol oxidation as a catalytic surface probe. *Appl. Catal. A*, 1997, **148**, 213–252.
20. Sanchez, E., Lopez, T., Gomez, R., Bokhimi, Morales, A. and Novaro, O., Synthesis and characterization of sol–gel Pt/TiO<sub>2</sub> catalyst. *J. Solid State Chem.*, 1996, **122**, 309–314.
21. Johannessen, T. and Koutsopoulos, S., One-step flame synthesis of an active Pt/TiO<sub>2</sub> catalyst for SO<sub>2</sub> oxidation – A possible alternative to traditional methods for parallel screening. *J. Catal.*, 2002, **205**, 404–408.
22. Fernandez-Ibanez, P., Blanco, J., Malato, S. and De Las Nieves, F. J., Application of the colloidal stability of TiO<sub>2</sub> particles for recovery and reuse in solar photocatalysis. *Water Res.*, 2003, **37**, 3180–3188.
23. Bae, H. S., Lee, M. K., Kim, W. W. and Rhee, C. K., Dispersion properties of TiO<sub>2</sub> nano-powder synthesized by homogeneous precipitation process at low temperature. *Colloids Surf. A: Physicochem. Eng. Aspects*, 2003, **220**, 169–177.
24. Park, H. and Choi, W., Effects of TiO<sub>2</sub> surface on photocatalytic reactions and photoelectrochemical behaviors. *J. Phys. Chem. B*, 2004, **108**, 4086–4093.
25. Leong, Y. K. and Ong, B. C., Critical zeta potential and the Hamaker constant of oxides in water. *Powder Technol.*, 2003, **134**, 249–254.
26. Hunter, R. J., *Zeta potential in colloid science principles and applications*. Academic Press, London, 1981.